Molecular and Cellular Endocrinology 490 (2019) 15–20

Contents lists available at ScienceDirect

Molecular and Cellular Endocrinology

journal homepage: www.elsevier.com/locate/mce

Absence of the long noncoding RNA H19 results in aberrant ovarian STAR and progesterone production

Yong Chen[a,b,1], Jing Wang[b,c,1], Yanhong Fan[b,d], Chunrong Qin[b,e], Xi Xia[b,f], Joshua Johnson[g], Amanda N. Kallen[b,*]

[b] Department of Obstetrics, Gynecology, and Reproductive Sciences, Yale School of Medicine, New Haven, CT, USA
[a] Department of Human Anatomy and Histology, and Embryology, School of Basic Medical Sciences, Fujian Medical University, Fuzhou, Fujian Province, 350122, PR China
[c] Department of Oncology, Beijing Friendship Hospital, Capital Medical University, Beijing, 100050, PR China
[d] Reproductive Medical Center, Department of Obstetrics and Gynecology, Peking University Third Hospital, Beijing, 100191, PR China
[e] Center for Reproductive Medicine, Affiliated Shenzhen City Maternity and Child Healthcare Hospital of Southern Medical University, Shenzhen, 518000, PR China
[f] Peking University Shenzhen Hospital, PR China
[g] Division of Reproductive Sciences, Department of Obstetrics and Gynecology, University of Colorado Denver, Aurora, CO, 80045, USA

ARTICLE INFO

Keywords:
StAR
H19
let-7
Steroidogenesis
Progesterone
Long noncoding RNA
lncRNA
cAMP

ABSTRACT

The steroidogenic acute regulatory protein (STAR) governs the rate-limiting step in steroidogenesis, and its expression varies depending on the needs of the specific tissue. It is well known that tight control of steroid production is essential for multiple processes involved in reproduction. We recently showed that *Star* is regulated at the posttranscriptional level *in vitro* by H19 and let-7. Here we demonstrate that this novel regulatory mechanism is functional *in vivo*, regulated by cAMP, and that loss of H19 not only disrupts ovarian STAR but also results in altered progesterone production in an H19KO mouse model. This work further strengthens the possibility that noncoding-RNA-mediated regulation of STAR may play an important role in the regulation of steroid hormone production, and contributes further to our understanding of the many ways in which this important gene is regulated.

1. Introduction

Steroid hormones have broad physiologic roles and are essential for the regulation of a wide range of functions, including reproductive function and fertility. All steroid hormones are derived from cholesterol, which must first be transported from the outer mitochondrial membrane to the inner membrane of steroidogenic cells before it is converted to pregnenolone, the precursor of all steroids. This rate-limiting transport step of steroidogenesis is catalyzed by the steroidogenic acute regulatory protein (STAR). STAR is expressed in steroidogenic cells of the adrenal, testis and ovary, and it is essential for adrenal and gonadal cells steroidogenesis (Stocco and Clark, 1997).

Because of its crucial role in steroid hormone production, an understanding of the regulatory pathways controlling STAR expression is essential. Until now, the primary means of promoting STAR production has appeared to be via activation of transcription factors, via trophic-hormone-driven stimulation of the cAMP signaling pathway, though other mechanisms for regulation of STAR have been described (Clark et al., 1995). However, we recently showed that both human and mouse *Star* are also regulated posttranscriptionally by the long noncoding RNA H19 *in vitro* (Men et al., 2017). These observations represent the first report of STAR expression being regulated by noncoding RNA. *H19* is abundantly expressed in the early stages of embryogenesis and in adult tissues including skeletal muscle, heart (Gabory et al., 2009), uterus, mammary gland and ovary (Adriaenssens et al., 1999; Ariel et al., 1997). However, whether H19-mediated regulation of *Star* plays a functional role *in vivo* in steroidogenic tissues has not yet been determined. We thus sought to determine whether this regulatory mechanism is functional *in vivo* in steroidogenic cells of the ovary, and to better understand how steroid hormone production may be altered in the absence of H19.

* Corresponding author. Department of Obstetrics, Gynecology, and Reproductive Sciences, 333 Cedar St, PO Box 208063, New Haven, CT, 06512, USA.
E-mail address: amanda.kallen@yale.edu (A.N. Kallen).
[1] These authors contributed equally to this work.

https://doi.org/10.1016/j.mce.2019.03.009
Received 10 July 2018; Received in revised form 20 March 2019; Accepted 20 March 2019
Available online 25 March 2019
0303-7207/

2. Materials and methods

2.1. Mouse strains and animal care

Homozygous $H19^{\Delta 3}$ loss-of-function mice were used for this study. The strain is maintained on a C57Bl/6J background and is characterized by deletion of the 3-kb transcription unit upstream of the *H19* gene itself (Gabory et al., 2009; Ripoche et al., 1997). Controls for H19KO females were homozygous wild-type (WT) C57Bl/6J littermates. Animals were maintained and euthanized according to principles and procedures described in the National Institutes of Health *Guide for the Care and Use of Laboratory Animals*. These studies were approved by the Yale University Institutional Animal Care and Use Committee (IACUC) and conducted in accordance with the Society for the Study of Reproduction's specific guidelines and standards.

2.2. Cell culture

The human ovarian granulosa-like tumor cell line, KGN was obtained from a collaborator, Dr. Maria Lalioti. KGN cells are undifferentiated and maintain physiological characteristics of ovarian cells (Havelock et al., 2004), and we have utilized these cells successfully for H19 overexpression experiments (Men et al., 2017). KGN cells were cultured at 37 °C with 5% CO_2 in 24-well plates in 0.5 mL Dulbecco's minimal essential medium/F12 medium (Sigma-Aldrich, USA, #D6421) supplemented with 10% fetal bovine serum (Gibco, USA, #10438018) and 1% penicillin-streptomycin (Sigma-Aldrich, USA, #P4333) in 5% CO_2 at 37 °C.

The luteinized mouse granulosa cell line, KK1, was obtained from a collaborator, Dr. Nathalie Clemente. The KK1 cell line has a female karyotype, expresses steroidogenic enzymes and is gonadotropin-response (Kananen et al., 1995). KK1 cells were cultured at 37 °C with 5% CO_2 in 24-well plates in 500 µl Dulbecco's minimal essential medium/F12 medium (Sigma-Aldrich, USA, #D6421) supplemented with 10% fetal bovine serum (Gibco, USA, #10438018) and 1% penicillin-streptomycin (Sigma-Aldrich, USA, #P4333) in 5% CO_2 at 37 °C.

In order to obtain mouse primary granulosa cells, mature (5-wk old) H19KO WT C57/Bl6 female mice were superovulated by intraperitoneal injection of 5IU pregnant mare serum gonadotropin (PMSG) x 2 (Folligon, Sigma-Aldrich, USA, #G4877) to stimulate follicle development and allow collection of adequate GCs for culture (Torrealday et al., 2013). 24 h after the second injection, mice were given an injection of 5IU human chorionic gonadotropin (hCG, Sigma Aldrich) to mimic an endogenous LH surge and trigger GC luteinization and STAR production. 16 h after hCG, mice were euthanized and GCs were isolated by puncturing the ovaries with a 26.5-gauge needle under a dissecting microscope (Olympus SZH-ILLK). GCs were separated from surrounding cells and tissues using a 0.40-µm strainer and spun down for 5 min at 1500 × *g*, then resuspended in 500 µL α-MEM (Sigma Aldrich, USA, #8042) supplemented with 5% fetal bovine serum (Gibco, USA, #10438018) and 1% penicillin-streptomycin (Sigma-Aldrich, USA, #P4333) in 24-well plates at 37 °C with 5% CO_2 to approximately 60–80% confluency.

2.3. Transfection and cAMP stimulation

In order to evaluate the effect of H19 overexpression on progesterone production, we performed H19 transfection in KGN cells utilizing the H19 expression vector $pH19^{11}$. H19 transfection was performed by mixing 0.2 µg H19 plasmid DNA or empty vector plasmid per well with 25 µl OPTI-MEM reduced serum medium (Thermo-Fisher Scientific, USA, #31985062) per well by gentle pipetting (Men et al., 2017). In parallel, 2 µl of lipofectamine 2000 (Thermo-Fisher Scientific, USA, #11668027) per well was mixed with 25 µl of OPTI-MEM per well. Following 5 min of incubation at room temperature, the two were mixed by gentle pipetting and incubated for 20 min at RT to allow plasmid/lipid complexes to form. At the end of incubation, the 50 µl/well transfection solution was used to re-suspend the cell pellet (5×10^5 cells/well). After incubation at room temperature for 10 min, regular growth medium was added at a ratio of 1:3 with and without 1 mM N6,2-dibutyryladenosine-3,5-cyclic monophosphate (dbcAMP, Sigma-Aldrich, USA, #D0627), and the cell suspension was transferred to the culture plate. After 24 h incubation at 37 °C in 5% CO_2, the medium was replaced with fresh growth medium and dbcAMP. RNA was extracted 48 h after transfection and RNA levels determined by RT-qPCR as described in the following subsection. Cells were transfected in a 48-well plate scale. Results are representative of three independent transfection experiments, evaluated as technical duplicates.

Since H19 expression is low in KGN cells, we turned to KK1 cells in order to perform H19 knockdown (Men et al., 2017; Kallen et al., 2013). For these experiments, 25 pmol of mouse-specific siH19 (simH19, ThermoFisher Scientific, USA, #4390771) or siCON (containing negative control siRNAs with no sequence similarity to mouse gene sequences) (ThermoFisher Scientific, USA, #4404020) was mixed with 50 µl OPTI-MEM per well by gentle pipetting. In parallel, 1.25 µl of lipofectamine 2000 per well was mixed with 50 µl of OPTI-MEM per well. Following 5 min of incubation at room temperature, the two were mixed by gentle pipetting and incubated for 20 min at RT to allow siRNA/lipid complexes to form. At the end of incubation, cells were resuspended in the transfection solution and growth medium was added with and without dbcAMP as above. RNA was extracted 48 h after transfection and H19 and *Star* RNA levels determined by RT-qPCR as described in the following subsection. Cells were transfected in a 48-well plate scale. Results are representative of three independent transfection experiments, evaluated as technical duplicates.

2.4. Reverse transcription, real-time PCR, and Western blot

RT-qPCR was performed to assess ovarian H19 levels at baseline across the WT mouse estrus cycle, as well as to evaluate STAR mRNA levels after H19 knockdown and overexpression *in vitro* (Men et al., 2017; Kallen et al., 2013). Primers for H19, *Star,* and beta-tubulin (used as a housekeeping gene) were purchased from the Yale University W.M. Keck Oligonucleotide Synthesis Facility (USA). For ovarian H19 expression, mouse ovaries were collected from 8 to 12 week WT mice. cDNA was synthesized using Bio-Rad iSCRIPT kit (Thermo-Fisher, USA, #1708841) in a 20 µl reaction containing 0.5 µg of total RNA. qPCR was performed in a 25 µl reaction containing 0.5–1.5 µl of cDNA using Bio-Rad iQSYBRGreen kit (Thermo-Fisher, USA, #1725150) in a Bio-Rad iCycler. PCR was performed by initial denaturation at 95 °C for 5 min, followed by 40 cycles of 30 s at 95 °C, 30 s at 60 °C, and 30 s at 72 °C. To assess STAR mRNA levels after H19 knockdown and overexpression *in vitro,* transfection was performed as described in the previous subsection, followed by cDNA synthesis and qRT-PCR. All primers had an efficiency of > 90%. All SYBR green runs had dissociation curves to predict potential primer-dimers. Specificity was verified by melting curve analysis and agarose gel electrophoresis. The threshold cycle (Ct) values of each sample were used in the post-PCR data analysis, and the delta-delta Ct method was used to calculate mRNA levels (Pfaffl, 2001). The PCR primers for the indicated human and mouse genes are listed below.

Human H19 forward: 5′-GCACCTTGGACATCTGGAGT.
Human H19 reverse: 5′-TTCTTTCCAGCCCTAGCTCA.
Mouse H19 forward: 5′-CCTCAAGATGAAAGAAATGGTGCTA-3′
Mouse H19 reverse: 5′-TCAGAACGAGACGGACTTAAAGAA-3′
Human STAR forward: 5′-GGCATCCTTAGCAACCAAGA.
Human STAR reverse: 5′-TCTCCTTGACATTGGGGTTC.
Mouse STAR forward: 5′-TTGGGCATACTCAACAACCA.
Mouse STAR reverse: 5′-GAAACACCTTGCCCACATCT.
Human/mouse beta-tubulin forward: 5′-CGTGTTCGGCCAGAGTGG TGC.
Human beta-tubulin reverse: 5′-GGGTGAGGGCATGACGCTGAA.

We then performed Western blot to measure STAR protein levels (Men et al., 2017). In brief, cells were harvested and cell pellets directly lysed in 3 vol of 2X SDS-sample buffer by heating at 95 °C for 5 min with occasional vortexing to break chromosomal DNA. Cell lysates (5–10 μl/well) were resolved on 10% SDS-PAGE, followed by Western blot analysis using rabbit StAR primary antibody (rabbit monoclonal, Cell Signaling, USA, #8449, 1:1000 dilution) and goat anti-rabbit secondary antibody (1:2000). For assessment of protein levels in whole ovary, mice were euthanized and whole ovaries harvested. Western blot was performed on whole ovary lysates as described above. β-actin primary antibody (mouse monoclonal, Sigma Aldrich, USA, #0198, 1:2000 dilution) and tubulin primary antibody (mouse monoclonal, Sigma Aldrich, USA, #0198, 1:2000 dilution) were used as controls. Western blot quantifications were performed using ImageJ.

2.5. Progesterone quantification

Mouse estrus cycle staging was performed by a single trained laboratory member (Y.Chen) via assessment of vaginal smear cytology (Caligioni, 2009). Retroorbital blood collection was performed at each estrus cycle stage, from alternating eyes at an interval of no less than 7 days per eye. Sera were prepared by clotting blood for 60–90 min at room temperature (RT).

Supernatants were recovered by centrifugation at RT for 10–15 min at 2000g. Sera samples were frozen at −20 until progesterone quantification was performed. ELISA for serum progesterone was performed per kit-specific protocol. The progesterone (P) ELISA kit (Cayman Chemical, USA, #582601) has a range of 7.8–1000 pg/mL and a sensitivity (80% B/B_0) of 10 pg/mL. The intra-assay CV was 9.6% and the inter-assay CV was 11%. Mean absorbance of the standards was plotted against concentration, and values of the samples on the standard curve interpolated to obtain the corresponding values of the concentrations. Serial dilutions of samples were performed in duplicate. Analyses were performed from 5 biological replicates per group, per estrus cycle stage, evaluated as technical duplicates. For *in vitro* P assays, progesterone concentration was determined after 24 h of culture (for mouse granulosa cells) and normalized to total RNA. Lastly, 48 h after transfection and H19 overexpression, P concentration was determined as above and results normalized to total RNA. Analyses were performed from 3 biological replicates per group, evaluated as technical duplicates.

2.6. Statistical analysis

Data were analyzed using GraphPad. Student's t-test or two-way ANOVA was used to calculate p values, and multiple comparisons were corrected by the Tukey method. P-values of 0.05 or less were considered statistically significant. Data presented as mean ± SE.

3. Results

3.1. H19 regulates STAR and progesterone production in cultured granulosa cells

We first sought to determine whether H19 expression affects the production of STAR in mouse granulosa cells. In order to achieve this aim, we performed Western blot for STAR as described above. As expected, decreased STAR was observed in H19KO mouse granulosa cells as compared to WT (Fig. 1a, Western blot, compare top left to top right bands; and Fig. 1b, demonstrating quantification of Western blot; $*p < 0.05$). We then sought to determine whether loss of H19 in these cultured granulosa cells would affect progesterone production. Progesterone production was decreased in GCs from H19KO mice as compared to WT (Fig. 1c, compare left to right bar, $**p < 0.01$).

We then evaluated progesterone production in cultured GCs after H19 overexpression in the presence and absence of cAMP. H19 overexpression in GCs resulted in increased progesterone production compared to vector control (Fig. 2, compare 3rd bar from left to 1st bar from left, $**p < 0.01$). As expected, treatment with cAMP also increased progesterone production (Fig. 2, compare 2nd bar from left to 1st bar from left, $**p < 0.01$). cAMP stimulation of cells expressing high levels of H19 increased progesterone production beyond levels seen after cAMP stimulation or H19 expression alone (Fig. 2, compare 4th bar from left with 2nd and 3rd bar from left, $**p < 0.01$). P values were calculated using two-way ANOVA and multiple comparisons were corrected by the Tukey method. $n = 3$, $* = p < 0.05$; $** = p < 0.01$.

3.2. STAR and progesterone are altered in H19KO mice

In order to determine whether absence of H19 disrupts the normal cyclicity of STAR and progesterone production across the mouse estrus cycle, we evaluated *STAR* protein production and serum progesterone level fluctuations by estrus stage in H19KO mice. Interestingly, a total dysregulation of STAR was seen in H19 KO mice as compared to WT mice (Fig. 3a, quantified in 3b). In WT mice, ovarian STAR and P production exhibited an expected peak in metestrus, immediately after ovulation typically occurs (Butts et al., 2010). However, in H19KO mice, STAR was nearly absent for half of the mouse estrus cycle, including during metestrus (Fig. 3a). Moreover, P levels remained comparatively low in H19KO mice as compared to WT mice across the estrus cycle, with no post-ovulatory peak observed (Fig. 3c, $*p < 0.05$). Lastly, we confirmed previous reports demonstrating H19 expression in mouse ovaries (Fig. 3d).

3.3. cAMP stimulates both H19 and star, and absence of H19 blunts cAMP-dependent star stimulation

Treatment with cAMP increased *Star* mRNA expression approximately fourfold, as expected, in cultured GCs, and increased H19 mRNA expression approximately twofold (Fig. 4). After H19 knockdown was performed in cultured GCS, H19 mRNA expression was markedly decreased (in comparison to treatment with scrambled sequence siRNA (siCon)). Lastly, GCs were treated with siCON or siH19 and then stimulated with cAMP. After H19 knockdown, cAMP treatment resulted in a blunting of peak *Star* mRNA expression levels as compared to siCON treatment (Fig. 4).

4. Discussion

Noncoding RNAs (ncRNAs) such as H19 have emerged as master regulators of tissue growth and differentiation. However, until our work, the role of long ncRNAs in particular in steroidogenesis has remained relatively unexplored. We recently showed that STAR is regulated at the posttranscriptional level *in vitro* by H19 and let-7. Here we demonstrate that H19 is present in the mouse ovary across the estrus cycle, and that loss of *H19 in vitro* and *in vivo* results in disrupted STAR production and progesterone synthesis, and that loss of *H19 in vitro* blunts peak cAMP-stimulated STAR expression. While transcription-independent regulation of STAR has been described (Ronen-fuhrmann et al., 1998), to our knowledge this is the first report of lncRNA-mediated STAR production.

At the molecular level, STAR expression in the ovary follows a cyclic, biphasic pattern. An initial small increase in STAR expression is observed in preovulatory interstitial and theca cells of the ovary (though overall STAR protein levels remain low), a process thought to drive androgen production in this ovarian compartment (Ronen-fuhrmann et al., 1998). GCs synthesize estradiol from these androgen precursors, a process which is STAR-independent; hence, STAR expression is not observed in GCs at this point in the cycle (Ronen-fuhrmann et al., 1998). The onset of the LH surge triggers ovulation, at which time GC STAR expression, and thus progesterone synthesis, is dramatically upregulated (Ronen-fuhrmann et al., 1998). Intriguingly, a cyclic pattern to H19 expression - quite similar to that of STAR - has been observed. In

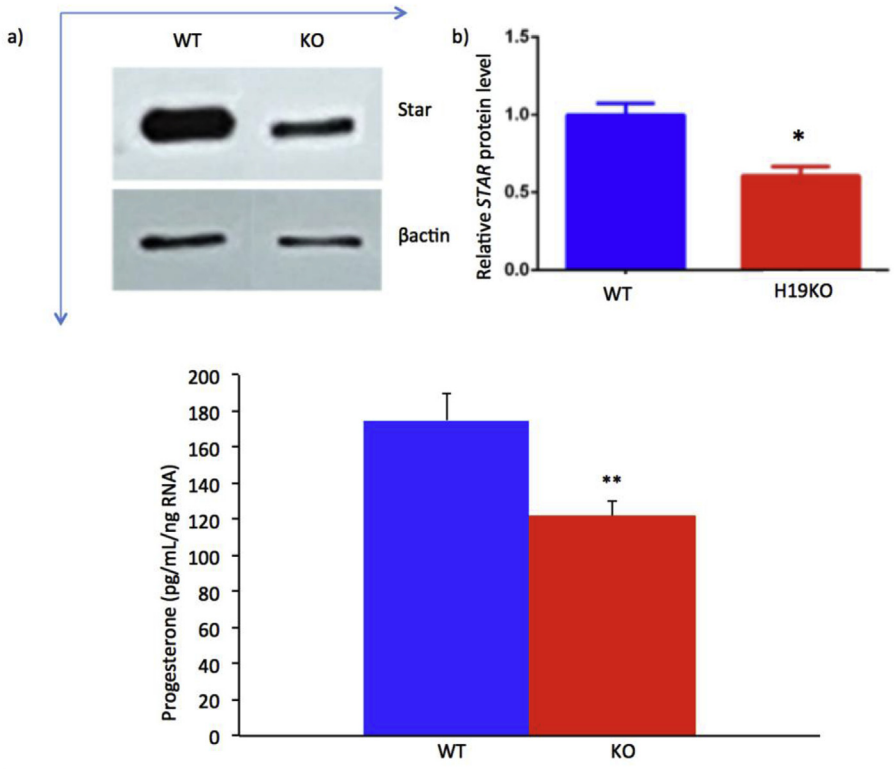

Fig. 1. Decreased *STAR* expression and progesterone in primary granulosa cells of H19KO mice. a) 5 week old H19KO and WT C57/Bl6 female mice (n = 3 per group) were superovulated by intraperitoneal injection of 5IU pregnant mare serum gonadotropin (PMSG) x 2 to stimulate follicle development. 24 h after the second injection, mice were given an injection of 5IU hCG, and GCs were isolated 16 h later and cultured in α-MEM. After 24 h of culture, Western blot was performed to measure STAR protein levels, using β-actin as control. Decreased *STAR* was observed in primary GCs from H19KO mice as compared to WT. b). Quantification of Western blot showing decreased *STAR* expression; $p < 0.05$. c) Progesterone concentration was determined via ELISA after 24 h of culture and normalized to total RNA. Progesterone production from cultured H19KO GCs was decreased as compared to WT GCs. $p < 0.01$. All data were analyzed using Student's t-test. *$p < 0.05$; **$p < 0.01$.

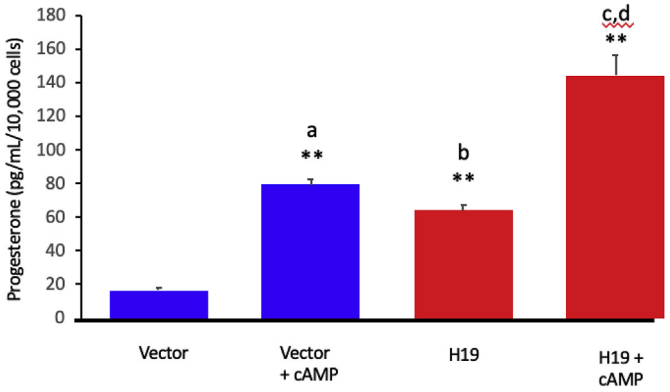

Fig. 2. H19 overexpression increases progesterone production synergistically with cAMP *in vitro*. H19 overexpression was performed in KGN cells using empty vector plasmid as control. Cells were transfected in the presence and absence of dbcAMP (1 mm). 48 h after transfection, P concentration was determined by ELISA and results normalized to total RNA. The progesterone yield after H19 overexpression in KGN cells (third bar from left) normalized to cell number was comparable to that observed after cAMP stimulation (second bar from left), and H19 overexpression plus cAMP yielded additive effects on progesterone production (fourth bar from left). Analyses were performed from 3 biological replicates per group, evaluated as technical duplicates. P values were calculated using two-way ANOVA and multiple comparisons were corrected by the Tukey method. n = 3, * = $p < 0.05$; ** = $p < 0.01$. a = vector +cAMP vs vector; b = H19 vs vector; c = H19 vs H19 + cAMP; d = vector +cAMP vs H19 + cAMP. n = 3; **$p < 0.01$.

particular, prominent and uniform H19 expression was observed in TCs of mature (antral) preovulatory follicles, and H19 expression became detectable in GCs after ovulation (Ariel et al., 1997). Intriguingly, this pattern - expression in TCs prior to ovulation, and in GCs after ovulation – mimics that of STAR. It also remains to be seen whether alterations in steroidogenesis in H19KO mice extend to other steroid hormones beyond progesterone, as would be expected if STAR production is altered, and to other steroidogenic enzymes in addition to STAR. The possibility that H19 could play a more global role in regulating steroidogenic cells is an intriguing one and future work will seek to further clarify this question.

A notable observation from our data is that STAR, while markedly decreased in metestrus mouse ovaries, is not absent. This may be attributable to the fact that the regulation of ovarian STAR expression is complex, and dependent on many factors in addition to H19. STAR expression depends on estrus cycle stage and cell type, and is detectable in theca-interstitial cells during follicular development (proestrus/estrus), with an increasing contribution from granulosa cells after ovulation (metestrus) (Ronen-fuhrmann et al., 1998; Green, 1966). This temporal pattern of expression is primarily regulated by circulating gonadotropins (which activate the cAMP/PKA signaling pathway and promote induction of transcription factors involved in the regulation of *Star* expression) but additional non-cAMP-driven pathways for *Star* regulation exist, including those involving vasoactive intestinal peptide (Kowalewski et al., 2010), epidermal growth factor and insulin-like growth factor 1 (Manna et al., 2002, 2006), arachidonic acid (Wang et al., 2006), and chloride and calcium ions (Ramnath et al., 1997). Whether any of these other regulatory pathways also may be affected by loss of H19 expression in *H19KO* mice is not known. However, because many factors regulate STAR in addition to H19, it is not surprising that the H19KO mouse ovary retains some (albeit abnormal) STAR production. The regulation of H19 itself is also poorly understood, and additional factors which remain unknown may contribute to the suprising patterns observed in H19KO mice.

It is also notable that the pattern of progesterone production observed in H19KO mice does not cause a marked impairment in fertility, although we previously showed that these mice exhibit a small but significant decrease in litter size at earlier reproductive ages, as well as accelerated follicular recruitment, compared to WT mice (Qin et al., 2018). The minimum amount of progesterone production necessary for pregnancy in rodents has been reported to be as low as 20–25% of normal, with no effect on implantation, embryo survival or fetal/placental growth (Elbaum et al., 1975; Milligan and Finn, 1997). Gidley-Baird et al. (Gidley-Baird, 1977) reported progesterone levels as low as

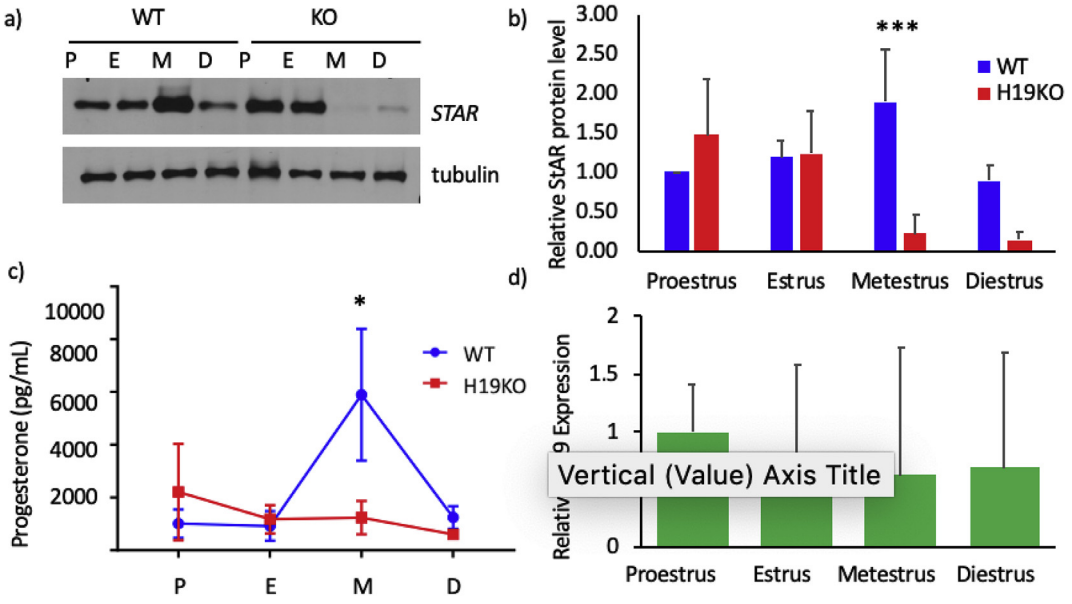

Fig. 3. Dysregulation of STAR expression and progesterone production in H19KO mice. STAR expression and progesterone levels were evaluated in 8 week H19KO and WT mice (n = 5 per group at each estrus cycle stage). Mouse estrus cycle staging was performed via assessment of vaginal smear cytology. a) For assessment of STAR protein levels, whole ovaries were harvested at each estrus cycle stage, and Western blot was performed on whole ovary lysates. *STAR* protein production was abnormal in H19KO mouse ovaries as compared to WT. In WT mice (left four lanes), ovarian *STAR* production peaks at metestrus. In H19KO mice (right four lanes), *STAR* expression is highest early in the mouse estrus cycle (proestrus and estrus), and nearly absent in metestrus and diestrus. b) Quantification of Western blots from all animals (n- = 5) depicted in a), showing *STAR* protein production changes over the estrus cycle in WT and H19KO mice. *p < 0.001. c) Retroorbital blood collection was performed at each estrus cycle stage, and serum progesterone quantified with ELISA. Serum progesterone levels in H19KO mice were altered as compared to WT. In WT mice, serum progesterone production peaks during metestrus. In H19KO mice, progesterone production remains markedly lower compared to WT mice with no "peak" in progesterone seen. P values were calculated using two-way ANOVA and multiple comparisons were corrected by the Tukey method. n = 3, * = p < 0.05; ** = p < 0.01. n = 5 per estrus stage, per group (WT and H19KO) * = p < 0.05. P = proestrus; E = estrus; M = metestrus; D = diestrus. WT = wild type. KO=H19 KO. d) To evaluate estrus cycle ovarian H19 expression, mouse ovaries were collected from 8 to 12 week WT mice (n = 5 per estrus cycle stage), and RNA extraction, cDNA synthesis and qRT-PCR were performed. Mean relative H19 expression levels by real-time PCR are shown, with results corrected to beta-tubulin. Error bars represent one SEM.

1 ng/mL (1000 pg/mL) in the five days prior to implantation, which approximates the minimum levels observed in our nonpregnant mice. However, progesterone requirements appear to change as pregnancy progresses (Milligan and Finn, 1997), and our study did not evaluate progesterone levels throughout implantation and early pregnancy in H19KO mice; thus it is not yet possible to say whether aberrant progesterone production persists throughout pregnancy, or if compensatory mechanisms exist to allow for minimum progesterone production throughout this period.

Our previously published work provides plausible mechanistic insight into *H19*-mediated regulation of STAR. We previously showed that *H19* sequesters the microRNA (miRNA) let-7, a small molecule that predominantly functions to silence target genes (Kallen et al., 2013). *H19,* by binding let-7, thus modulates its availability and leads to derepression of let-7 target genes. We also identified *Star* as a novel target of let-7[3], a finding which provides mechanistic insight into the method

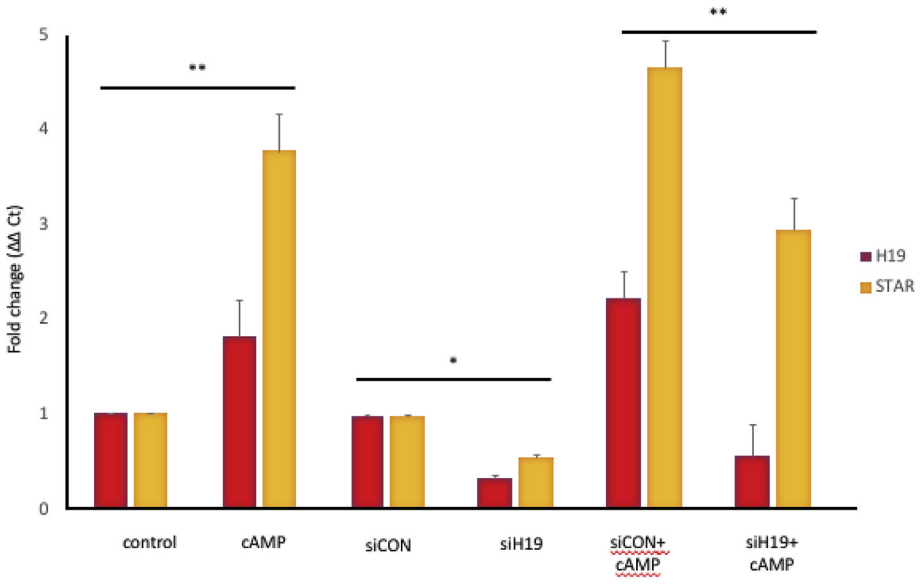

Fig. 4. cAMP-stimulated H19 and *Star* expression is decreased after H19 KD. KK1 cells were transfected with mouse-specific siH19 or negative control siRNA (siCon) in the presence and absence of dbcAMP (1 mM). RNA was extracted 48 h after transfection and H19 and *Star* RNA levels determined by RT-qPCR. cAMP treatment significantly increased both H19 and *Star* (**p < 0.01). cAMP-stimulated *Star* expression is significantly blunted after H19KD (**p < 0.01). Results are representative of three independent transfection experiments, evaluated as technical duplicates. P values were calculated using two-way ANOVA and multiple comparisons were corrected by the Tukey method. n = 3, * = p < 0.05; ** = p < 0.01.

by which H19 can regulate *Star*. Notably, in our prior work, let-7 levels themselves were not significantly altered in H19-expressing cells, suggested altered let-7 function without changes in let-7 levels or degradation of let-7 itself (Kallen et al., 2013).

In conclusion, our work demonstrates a novel mechanism by which STAR is regulated at the post-transcriptional level *in vivo* by non-coding RNAs, in particular H19, and cAMP-driven STAR stimulation may in fact be at least partially dependent on the upregulation of H19. To our knowledge, this work represents the first example of lncRNA-mediated control of the rate-limiting step of steroidogenesis, and thus adds to the body of literature describing the multiple roles in oncogenesis, cellular growth, glucose metabolism, and now regulation of steroidogenesis, of this complex lncRNA.

Disclosure statement

The authors have nothing to disclose.

Funding

The authors gratefully acknowledge funding and research support provided by the Reproductive Scientist Development Program (NIH-NICHD Project #2K12HD000849-26), the American Society for Reproductive Medicine, the NIH Loan Repayment Program, and the Milstein Medical Asian American partnership Foundation (MMAAPF), as well as H19 KO mice provided by Luisa Dandolo, PhD, and Stefan Muljo, PhD, and technical support provided by Yingqun Huang, MD, PhD.

References

Adriaenssens, E., Lottin, S., Dugimont, T., et al., 1999. Steroid hormones modulate H19 gene expression in both mammary gland and uterus. Oncogene 18 (31), 4460–4473. https://doi.org/10.1038/sj.onc.1202819.

Ariel, I., Weinstein, D., Voutilainen, R., et al., 1997. The expression of the imprinted gene H19 in the human female reproductive organs. Diagn. Mol. Pathol. 61 (1), 17–25.

Butts, C.L., Candando, K.M., Warfel, J., Belyavskaya, E., D'Agnillo, F., Sternberg, E.M., 2010. Progesterone regulation of uterine dendritic cell function in rodents is dependent on the stage of estrous cycle. Mucosal Immunol. 3 (5), 496–505. https://doi.org/10.1038/mi.2010.28.

Caligioni, C.S., 2009. Assessing reproductive status/stages in mice. Curr Protoc Neurosci 1–11. https://doi.org/10.1002/0471142301.nsa04is48. SUPPL. 48.

Clark, B.J., Soo, S.C., Caron, K.M., Ikeda, Y., Parker, K.L., Stocco, D.M., 1995. Hormonal and developmental regulation of the steroidogenic acute regulatory protein. Mol. Endocrinol. 9 (10), 1346–1355. https://doi.org/10.1210/mend.9.10.8544843.

Elbaum, D., Bender, E., Brown, J., Keyes, L., 1975. Serum progesterone in pregnant rats with corpora lutea: correlation ectopic or in situ of luteal tissue and progesterone concentration. Biol. Reprod. 13, 541–545.

Gabory, A., Ripoche, M.-A., Le Digarcher, A., et al., 2009. H19 acts as a trans regulator of the imprinted gene network controlling growth in mice. Development 136 (20), 3413–3421. https://doi.org/10.1242/dev.036061.

Gidley-Baird, A.A., 1977. Plasma progesterone, FSH and LH levels associated with implantation in the mouse. Aust. J. Biol. Sci. 30 (4), 289–296. https://doi.org/10.1071/BI9770289.

Green, E.L. (Ed.), 1966. Biology of the Laboratory Mouse, second ed. Dover Publications, Inc., New York, NY.

Havelock, J.C., Rainey, W.E., Carr, B.R., 2004. Ovarian granulosa cell lines. Mol. Cell. Endocrinol. 228 (1–2), 67–78. https://doi.org/10.1016/j.mce.2004.04.018.

Kallen, A.N., Zhou, X.B., Xu, J., et al., 2013. The imprinted H19 LncRNA antagonizes let-7 MicroRNAs. Mol. Cell 52 (1), 101–112. https://doi.org/10.1016/j.molcel.2013.08.027.

Kananen, K., Markkula, M., Rainio, E., Su, J.-G.G., Hsueh, A.J., Huhtaniemi, I.T., 1995. Gonadal tumorigenesis in transgenic mice bearing the mouse inhibin alpha-subunit promoter/simian virus T-antigen fusion gene: characterization of ovarian tumors and establishment of gonadotropin-responsive granulosa cell lines. Mol. Endocrinol. 9 (5), 616–627. https://doi.org/10.1210/mend.9.5.7565808.

Kowalewski, M.P., Dyson, M.T., Boos, A., Stocco, D.M., 2010. Vasoactive intestinal peptide (VIP)-mediated expression and function of steroidogenic acute regulatory protein (StAR) in granulosa cells. Mol. Cell. Endocrinol. 328 (1–2), 93–103. https://doi.org/10.1016/j.mce.2010.07.018.

Manna, P.R., Huhtaniemi, I.T., Wang, X.-J., Eubank, D.W., Stocco, D.M., 2002. Mechanisms of epidermal growth factor signaling: regulation of steroid biosynthesis and the steroidogenic acute regulatory protein in mouse leydig tumor cells. Biol. Reprod. 67 (5), 1393–1404. https://doi.org/10.1095/biolreprod.102.007179.

Manna, P.R., Chandrala, S.P., King, S.R., et al., 2006. Molecular mechanisms of insulin-like growth factor-I mediated regulation of the steroidogenic acute regulatory protein in mouse leydig cells. Mol. Endocrinol. 20 (2), 362–378. https://doi.org/10.1210/me.2004-0526.

Men, Y., Fan, Y., Shen, Y., Lu, L., Kallen, A.N., 2017. The steroidogenic acute regulatory protein (StAR) is regulated by the H19/let-7 axis. Endocrinology 158 (2), 402–409. https://doi.org/10.1210/en.2016-1340.

Milligan, S.R., Finn, C.A., 1997. Minimal progesterone support required for the maintenance of pregnancy in mice. Hum. Reprod. 12 (3), 602–607. https://doi.org/10.1093/humrep/12.3.602.

Pfaffl, M.W., 2001. A new mathematical model for relative quantification in real-time RT-PCR. Nucleic Acids Res. 29 (9), 45e–45. https://doi.org/10.1093/nar/29.9.e45.

Qin, C., Xia, X., Fan, Y., et al., 2018. A novel, noncoding-RNA-mediated, post-transcriptional mechanism of anti-Mullerian hormone regulation by the H19/let-7 axis†. Biol. Reprod. 0 (August), 1–11. https://doi.org/10.1093/biolre/ioy172.

Ramnath, H.I., Peterson, S., Michael, A.E., Stocco, D.M., Cooke, B.A., 1997. Modulation of steroidogenesis by chloride ions in MA-10 mouse tumor Leydig cells: roles of calcium, protein synthesis, and the steroidogenic acute regulatory protein. Endocrinology 138 (6), 2308–2314. https://doi.org/10.1210/en.138.6.2308.

Ripoche, M.A., Kress, C., Poirier, F., Dandolo, L., 1997. Deletion of the H19 transcription unit reveals the existence of a putative imprinting control element. Genes Dev. 11 (12), 1596–1604. https://doi.org/10.1101/gad.11.12.1596.

Ronen-fuhrmann, T., Timberg, R., King, S.R., et al., 1998. Spatio-temporal expression patterns of steroidogenic acute regulatory protein (StAR) during follicular development in the rat ovary. Endocrinology 139 (1), 303–315.

Stocco, D.M., Clark, B.J., 1997. The role of the steroidogenic acute regulatory protein in steroidogenesis. Steroids 62 (1), 29–36.

Torrealday, S., Lalioti, M.D., Guzeloglu-Kayisli, O., Seli, E., 2013. Characterization of the gonadotropin releasing hormone receptor (GnRHR) expression and activity in the female mouse ovary. Endocrinology 154 (10), 3877–3887. https://doi.org/10.1210/en.2013-1341.

Wang, X., Shen, C.L., Dyson, M.T., et al., 2006. The involvement of epoxygenase metabolites of arachidonic acid in cAMP-stimulated steroidogenesis and steroidogenic acute regulatory protein gene expression. J. Endocrinol. 190 (3), 871–878. https://doi.org/10.1677/joe.1.06933.